THE JOURNAL OF THE ACOUSTICAL SOCIETY OF KOREA Vol.21, No.3E 2002. 9. pp. 112~118

Tuning Fork Modal Analysis and Sound Pressure Calculation Using FEM and BEM

Soon-Suck Jarng*, Je-Hyung Lee*
*Dept. of Information Control & Instrumentation, Chosun University, Korea
(Received 4 April 2002; accepted 26 August 2002)

Abstract

An unconstrained tuning fork with a 3-D model has been numerically analyzed by Finite Element Method (FEM) and Boundary Element Method (BEM). The first three natural frequencies were calculated by the FEM modal analysis. Then the trend of the change of the modal frequencies was examined with the variation of the tuning fork length and width. An formula for the natural frequencies-tuning fork length relationship were derived from the numerical analysis results. Finally the BEM was used for the sound pressure field calculation from the structural displacement data.

Keywords: *Tuning fork, FEM, BEM, Modal analysis, Sound pressure field*

I. Introduction

The tuning fork was firstly invented in England by Royal trumpeter John Shore in 1711[1]. A tuning fork has its natural (modal) frequencies according to its materialistic and structural fabrication. Even though the tuning fork has a long history, its modal and acoustic analysis has not performed much. The tuning fork itself is surprisingly unstudied in numerical approach. There are a few references about the tuning fork analysis in analytical approach in 1930s[2]. The numerical approach has been available only since Boundary Element Method (BEM) technique overcame its singularity problems[3,4]. There has been no evidence of application for the tuning fork analysis using the BEM with Finite Element Method (FEM). It is therefore very meaningful to apply the BEM with the FEM to the tuning fork analysis because the mechanical behavior of the tuning fork may be predicted using the FEM-BEM numerical techniques. Many questions about the tuning fork might be arisen; the variation of the tuning fork length, the effect of the tuning fork width size, the sound pressure intensity around the tuning fork and material aspects etc. This paper answers to some of those questions. An unconstrained tuning fork with a 3-D model has been numerically analyzed by the FEM and the BEM. The FEM is used for calculation of modal frequencies and modal shapes (displacements) while the BEM is used for calculation of sound pressure in the 3-D space generated by the tuning fork at the natural frequency. This paper deals with not only the analysis of the tuning fork but also the practical design of the tuning fork.

Corresponding author: Soon-Suck Jarng (ssjarng@mail.chosun.ac.kr)
Chosun University, 375 SeoSeok-Dong, Dong-Ku, Gwang-Ju, Korea

II. Numerical Methods

2.1. Finite Element Method (FEM)

The following equation (1) is the integral formulation

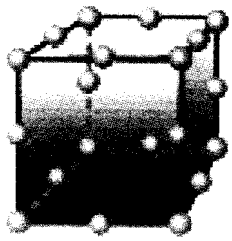

Figure 1. 3D quadratic hexahedral 20 nodes' element.

of the FEM elastic equations:

$$\{F\} = [K]\{a\} - \omega^2[M]\{a\} \tag{1}$$

where

$\{F\}$ Applied Mechanical Force
$\{a\}$ Elastic Displacement
$[K]$ Elastic Stiffness Matrix
$[M]$ Mass Matrix
ω Angular Frequency

The isoparametric formulation for 3-dimensional structural elements is well documented by Allik H. et. al.[5]. Each 3-dimensional finite element is composed of 20 quadratic nodes and each node has nodal displacement (a_x, a_y, a_z) variables. In local coordinates the finite element has 6 surface planes (±xy, ±yz, ±zx) which may be exposed to external air environment. The exposed surface is used as a boundary element which is composed of 8 quadratic nodes.

2.2. Boundary Element Method (BEM)

For sinusoidal steady-state problems, the Helmholtz equation, $\nabla^2\Psi + k^2\Psi = 0$ represents the fluid mechanics. Ψ is the acoustic pressure with time variation, $e^{j\omega t}$, and k(= ω/c) is the wave number. c is the sound speed, 340 [m/sec]. In order to solve the Helmholtz equation in an infinite air media, a solution to the equation must not only satisfy structural surface boundary condition (BC), $\partial\Psi/\partial n = -\rho_f\omega^2 a_n$ but also the radiation condition at infinity, $\lim_{r\to\infty}\oint_S(\partial\Psi/\partial r + jk\Psi)^2 dS = 0$. $\partial/\partial n$ represents differentiation along the outward normal to the boundary. ρ_f and a_n are the fluid density and the normal displacement on the structural surface. The Helmholtz integral equation derived from Green's second theorem provides such a solution for radiating pressure waves;

$$\oint_S\left(\Psi(q)\frac{\partial G_k(p,q)}{\partial n_q} - G_k(p,q)\frac{\partial\Psi(q)}{\partial n_q}\right)dS_q = \beta(p)\ \Psi(p) \tag{2}$$

where $G_k(p,q) = e^{-jkr}/4\pi r,\quad r = |p-q|$

In equation (2) p is any point in either the interior or the exterior and q is the surface point of integration. $\beta(p)$ is the exterior solid angle at p.

The acoustic pressure for the i^{th} global node, $\Psi(p_i)$, is expressed in discrete form[6];

$(1 \le i \le ng)$

$$\beta(p_i)\Psi(p_i) = \oint_S\left(\Psi(q)\frac{\partial G_k(p_i,q)}{\partial n_q} - G_k(p_i,q)\frac{\partial\Psi(q)}{\partial n_q}\right)dS_q \tag{3a}$$

$$= \sum_{m=1}^{nt}\int_{S_m}\left(\Psi(q)\frac{\partial G(p_i,q)}{\partial n_q} - G(p_i,q)\frac{\partial\Psi(q)}{\partial n_q}\right)dS_q \quad q\in S_m \tag{3b}$$

$$= \sum_{m=1}^{nt}\int_{S_m}\left(\sum_{j=1}^{8}N_j(q)\Psi_{m,j}\frac{\partial G(p_i,q)}{\partial n_q} - G(p_i,q)\sum_{j=1}^{8}N_j(q)\frac{\partial\Psi_{m,j}}{\partial n_q}\right)dS_q \tag{3c}$$

$$= \sum_{m=1}^{nt}\sum_{j=1}^{8}\left(\int_{S_m}N_j(q)\frac{\partial G(p_i,q)}{\partial n_q}dS_q\right)\Psi_{m,j} - \rho_f\omega^2\sum_{m=1}^{nt}\sum_{j=1}^{8}\left(\int_{S_m}N_j(q)G(p_i,q)n_q dS_q\right)a_{m,j} \tag{3d}$$

$$= \sum_{m=1}^{nt}\sum_{j=1}^{8}A^i_{m,j}\Psi_{m,j} - \rho_f\omega^2\sum_{m=}^{nt}\sum_{j=1}^{8}B^i_{m,j}a_{m,j} \tag{3e}$$

where nt is the total number of surface elements and $a_{m,j}$ are three dimensional displacements. Equation (3b) is derived from equation (3a) by discretizing integral surface. And equation (3c) is derived from equation (3b) since an acoustic pressure on an integral surface is interpolated from adjacent 8 quadratic nodal acoustic pressures corresponding the integral surface. Then equation (3d) is derived from equation (3c) by swapping integral notations with summing notations. Finally the parentheses of equation (3d) is expressed by upper capital notations for simplicity.

When equation (3e) is globally assembled, the discrete Helmholtz equation can be represented as

$$([A]-\beta[I])\{\Psi\}=+\rho_f\omega^2[B]\{a\} \tag{4}$$

where [A] and [B] are square matrices of (ng by ng) size. ng is the total number of surface nodes.

When the impedance matrices of equation (4), [A] and [B], are computed, two types of singularity arise[7]. One is that the Green's function of the equation, $G_k(p_i, q)$, becomes infinite as q approaches to p_i. This problem is solved by mapping such rectangular local coordinates into triangular local coordinates and again into polar local coordinates[8]. The other is that at certain wave number the matrices become ill-conditioned. These wave number are corresponding to eigenvalues of the interior Dirichlet problem[9]. One approach to overcome the matrix singularity is that [A] and [B] of equation (4) are modified to provide a unique solution for the entire frequency range [10-12]. The modified matrix equation referred to as the modified Helmholtz gradient formulation (HGF)[13] is obtained by adding a multiple of an extra integral equation to equation (4).

$$([A]-\beta[I]\oplus\alpha[C])\{\Psi\}=+\rho_f\omega^2([B]\oplus\alpha[D])\{a\} \tag{5}$$

where

$$\alpha=-\frac{\sqrt{-1}}{k\cdot(Nmber\ of\ surface\ element\ adjacent\ a\ surface\ node)}$$

[C] and [D] are rectangular matrices of (nt by ng) size. $\oplus$ symbol indicates that the rows of [C], [D] corresponding to surface elements adjacent to a surface node are added to the row of [A], [B] corresponding to the surface node, that is,

$$\sum_{i=1}^{ng}\sum_{j=1}^{ng}A(i,j)=\sum_{i=1}^{ng}\sum_{j=1}^{ng}A(i,j)+\sum_{i=1}^{ng}\sum_{j=1}^{ng}\left(\sum_{m=1}^{s(i)}\alpha\ \ C(m,j)\right)$$
$$\sum_{i=1}^{ng}\sum_{j=1}^{ng}B(i,j)=\sum_{i=1}^{ng}\sum_{j=1}^{ng}B(i,j)+\sum_{i=1}^{ng}\sum_{j=1}^{ng}\left(\sum_{m=1}^{s(i)}\alpha\ \ D(m,j)\right) \tag{6}$$

where S(i) is the number of surface element adjacent to a surface node. Equation (6) may be reduced in its formulation using superscript $\oplus$ for convenience;

$$A^{\oplus}\{\Psi\}=+\rho_f\omega^2B^{\oplus}\{a\} \tag{7}$$

where $([A]-\beta[I]\oplus\alpha[C])\equiv A^{\oplus}$, $([B]\oplus\alpha[D])\equiv B^{\oplus}$

Equation (7) can be written as

$$\{\Psi\}=+\rho_f\omega^2(A^{\oplus})^{-1}B^{\oplus}\{a\} \tag{8}$$

Since the present acoustic vibrator produces displacement data $\{a\}$ at a natural frequency, the surface pressure $\{\Psi\}$ of the tuning fork is calculated from equation (8). Once $\{a\}$ and $\{\Psi\}$ are known, the acoustic pressure in the near field is determined by $\beta(p)=1$ of equation (2) for given values of surface nodal pressure and surface nodal displacement;

$$\Psi(p_i)=\sum_{m=1}^{nt}\sum_{j=1}^{8}A^{i}_{m,j}\Psi_{m,j}-\rho_f\omega^2\sum_{m=1}^{nt}\sum_{j=1}^{8}B^{i}_{m,j}a_{m,j} \tag{9}$$

III. Results

The FEM and BEM have been programmed with Fortran language running at a PC with 2G RAM. Calculation is done with double precision and the program is made for three dimensional structures. Because each structural node has 3 DOF, the size of the globally assembled coefficient matrices of the matrix equation are 3*ng by 3*ng. The particular structure considered is an unconstrained tuning fork (Fig. 2). The whole tuning fork is modeled using 550 isoparametric elements. Global node numbers are 3934 nodes. It is desired to have more elements representing smaller local regions for higher frequency analysis. However, calculation with more number of nodes costs more time. Therefore meshing of elements depends on the maximal limit of interesting frequency. It is a common practice to have the size of the largest element to be less than $\lambda/3$[6]. In this paper the interest frequency of the acoustic radiation is less than 10,000 Hz,

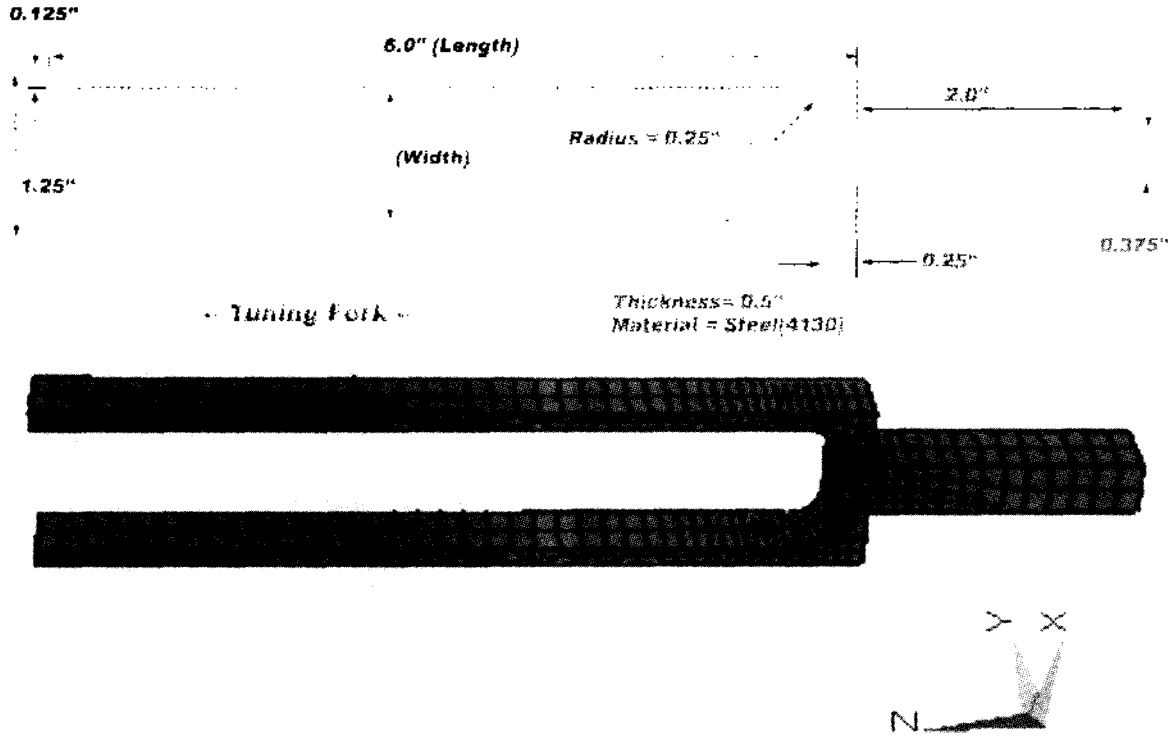

Figure 2. 3D tuning fork dimensions. Elements=550. Nodes=3934.

Table 1. Material properties.

	Density (ρ) [Kg/m^3]	Young's Modulus (E) [N/m^2]	Poisson Ratio (ν)
Air	1.22	1.411E5	-
Steel	7822.9	2.0684E11	0.30
Aluminum	2703.8	6.9637E10	0.36

so that $\lambda/3$ is about 11.3 mm.

Table 1 shows the material properties of the air, steel and aluminum. The first three natural frequencies were calculated from the FEM equation (1) where $\{F\}=0$. In modal analysis $\{a\}$ is an eigenvector and $\lambda\equiv(\omega^2)$ is an eigenvalue.

$$[K]\{a\} = \lambda[M]\{a\}(\equiv\omega^2[M]\{a\}) \tag{10}$$

Fig. 3 shows the modal shape of the tuning fork at 128.4 Hz (1st mode). The length and the width of the tuning fork are 152.4 [mm] and 25.4 [mm]. And the applied material is steel (4130). The green frame is the undeformed shape of the tuning fork while the solid color shows the Von Mises stress (Equation 11) with deformed shape.

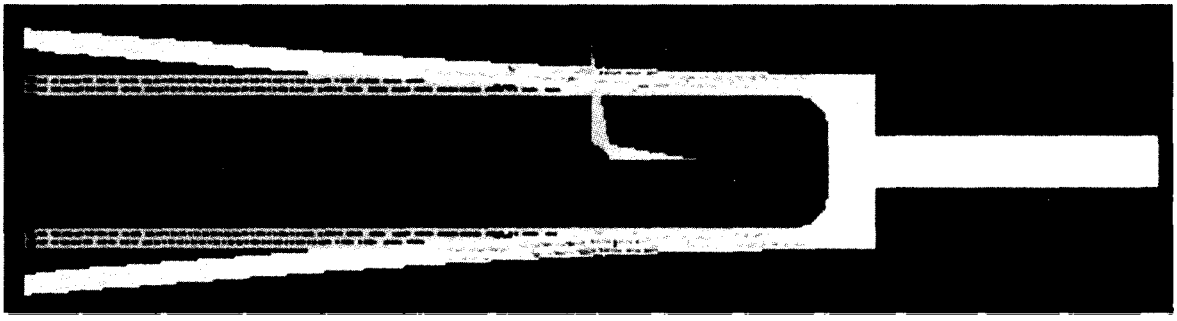

Figure 3. Modal shape of tuning fork (Color=Von Mises Stress) at 128.4 Hz (1st mode), Length=152.4 [mm], Width=25.4 [mm], Material =Steel(4130)

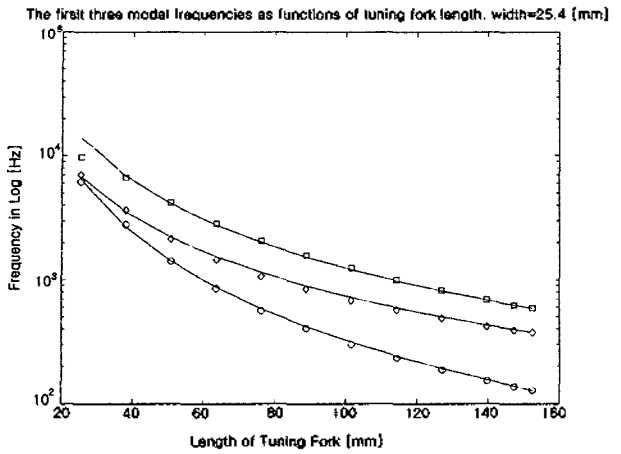

Figure 4. The first three modal frequencies as functions of tuning fork length.
Circle=1st mo+de, Diamond=2nd mode, Rectangle=3rd mode.

$$\sqrt{0.5[(\sigma_1-\sigma_2)^2+(\sigma_2-\sigma_3)^2+(\sigma_3-\sigma_1)^2]} \qquad (11)$$

where σ_1, σ_2, σ_3 are stresses in x, y, z coordinates.

Then the change of the modal frequencies was calculated with the variation of the tuning fork length and width. Fig. 4 shows the first three modal frequencies as functions of tuning fork length with a constant width. Each symbol indicates different modal frequencies (Circle=1st mode, Diamond=2nd mode, Rectangle=3rd mode). Modal frequencies are exponentially increased with the reduced size of the tuning fork length.

A relationship for the natural frequencies-tuning fork length were derived from the numerical analysis results (Table 2). Solid continuous lines of Fig. 4 were drawn from the analytical model equations for each mode. And Fig. 5 shows the comparison in percentage [%] between FEM results and model equations. The most significant difference happened at the 3rd mode with 25.4 [mm] tuning fork length, that is, 44%. But the rest of the results show less than 8% differences.

Table 3 shows that the change of the tuning fork width does not significantly affect of the modal frequencies. Also Fig. 6 shows that the modal frequencies of the tuning fork remain almost the same as Fig. 4 though the material is changed from steel (continuous line) to aluminum (dashed line). These results show that the length of the tuning fork mainly affects the natural frequencies of the tuning fork as far as metallic materials are used.

Table 4 compares of modal frequencies between the

Table 2. Analytical model equations for each tuning fork mode, x [m].

	1st Mode	2nd Mode	3rd Mode
Model Equations	$\frac{2.0859}{x^{2.19}}$	$\frac{17.759}{x^{1.82}}$	$\frac{21.040}{x^{1.77}}$

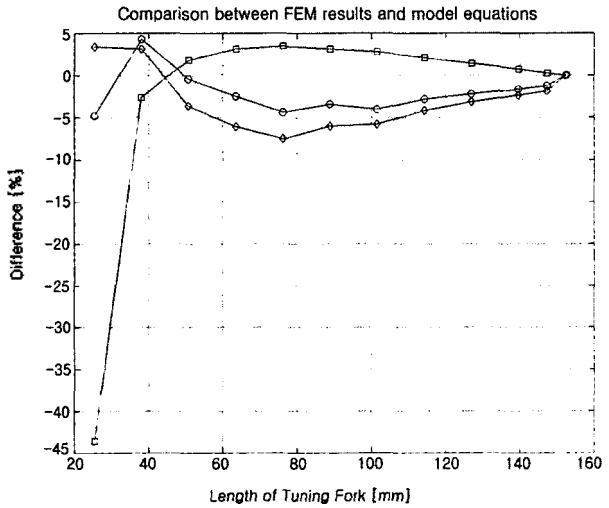

Figure 5. Comparison in percentage [%] between FEM results and model equations.
Circle=1st mode, Diamond=2nd mode, Rectangle=3rd mode.

Table 3. Modal frequencies with different tuning fork width Length=152.4 [mm], Material=Steel (4130).

Width [mm]	Frequency [Hz]		
	1st mode	2nd mode	3rd mode
50.8	93.5	198.9	525.2
38.1	125.6	339.5	559.5
25.4	128.5	374.1	587.7
12.7	128.6	391.2	576.7
6.3	124.2	395.2	525.5

Table 4. Comparison of modal frequencies between the present results and Algor results[14]. Length=152.4 [mm], Width=25.4 [mm], Material=Steel (4130).

Results	Frequency [Hz]		
	1st mode	2nd mode	3rd mode
Author's	128.5	374.1	587.7
Algor's	127.9	368.9	603.4
Difference	0.6	5.2	-15.4
%	0.5	1.4	2.7

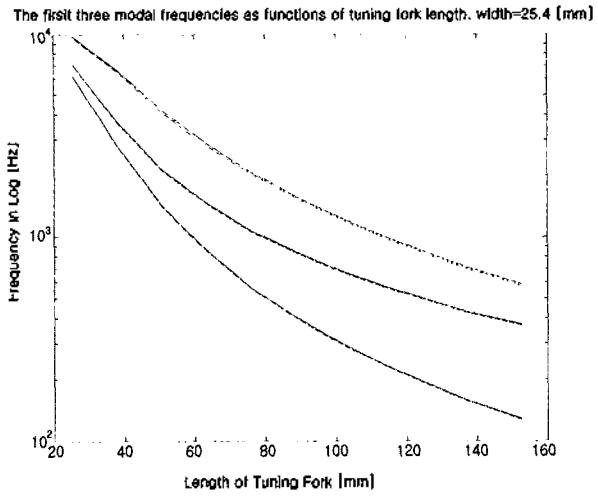

Figure 6. The first three modal frequencies as functions of tuning fork length as Fig. 4.
Continuous Lines=Steel. Dashed Lines=Aluminum.

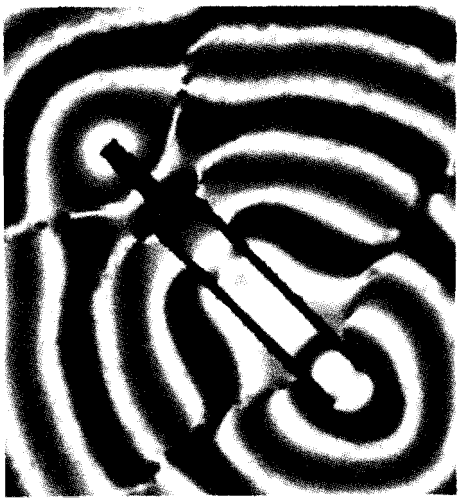

Figure 8. Acoustic pressure radiation pattern of Fig. 7.

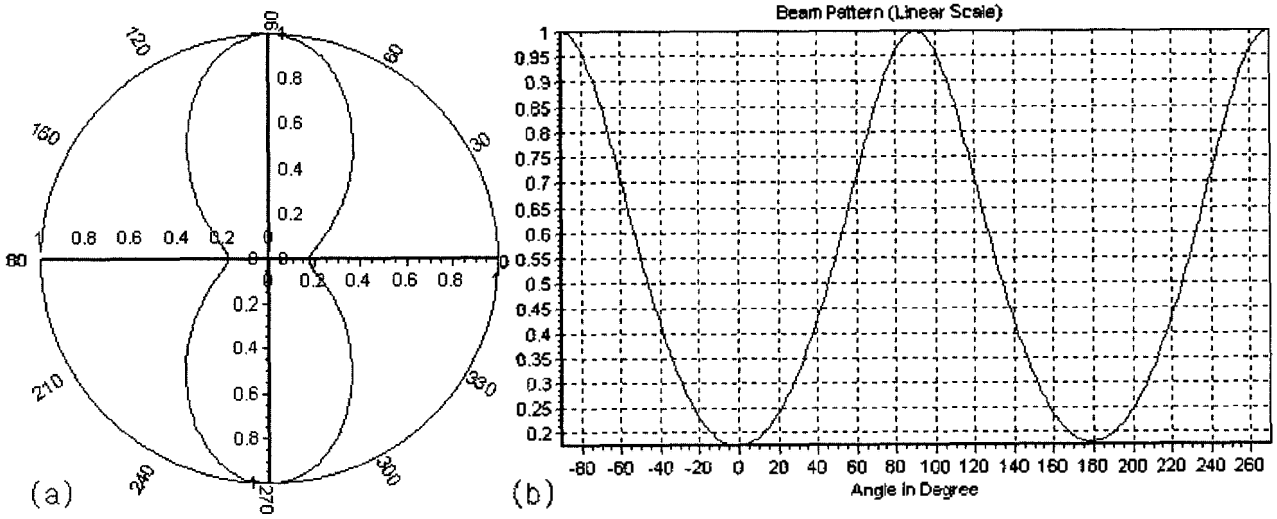

Figure 7. Acoustic pressure directivity pattern at 1 [m] away from the tuning fork. At 128.4 Hz (1st mode), Length=152.4 [mm], Width=25.4 [mm], Material=Steel (4130).

present results and Algor results[14]. The difference between two results slightly increased with higher modal frequency.

Finally the BEM was used for the sound pressure field calculation from the structural displacement data. From equation (9) the acoustic pressure in the near field is calculated along the circle with the directivity angle ϕ (Fig. 7). The normalized value of the near field pressure is used as the quantitative degree of the directivity. Fig. 7 shows the acoustic pressure directivity pattern at 1 [m] away from the tuning fork at 128.4 Hz (1st mode). Because the modal frequency is low, the directivity pattern is almost omni-directional. And Fig. 8 shows the acoustic pressure radiation pattern of Fig. 7[15].

IV. Conclusion

It is very meaningful to apply the BEM with the FEM to the tuning fork analysis because the mechanical behavior of the tuning fork may be numerically predicted using the FEM-BEM techniques. Even though the structure of the tuning fork is simple and is well known, its numerical

analysis is surprisingly undone. The quantitative analysis of the tuning fork in this paper suggests further numerical research of mechanically sound generating devices. That is, the geometry of the tuning fork can be changed as far as different functionality is concerned such as acoustic pressure radiation pattern. It is concluded that the length of the tuning fork mainly affects the natural frequencies of the tuning fork as far as metallic materials are used. The width of the tuning fork does not much produce differences in modal frequencies. Numerically formulated table can be used as the designing factor of the tuning fork fabrication. The length of the tuning fork may be changed for a desired first modal frequency such as A pitch (=440 Hz) etc. This work need to be further developed for a particular radiation pattern synthesis.

Acknowledgments

This study was supported by sabbatical research fund from Chosun University, 1999.

References

1. A. J. Ellis. "On the history of musical pitch," *Journal of the Society of Arts, March 5, 1880. Reprinted in Studies in the History of Music Pitch*, Amsterdam: Frits Knuf, p. 44. Ellis measured the pitch of the Streicher fork at A= 442.78, 1968.
2. O. H. Schuck, "An adjustable tuning frok frequency standard," *J. Acoust. Soc. Am.* **10**, 119-127, 1938.
3. M. R. Bai, "Application of BEM (boundary element method) -based acoustic holography to radiation analysis of sound sources with arbitrarily shaped geometries," *J. Acoust. Soc. Am.* **92** (1), 533-549, 1992.
4. C. S. Pates III, U. S. Shirahatti, C. Mei, "Sound-structure interaction analysis of composite panels using coupled boundary and finite element methods," *J. Acoust. Soc. Am.* **98** (2), 1216-1221, 1995.
5. H. Allik and T. J. R. Hughes, "Finite element method for piezoelectric vibration," *Int. J. Numer. Method Eng.*, 2, 151-157, 1970.
6. S. S. Jarng, "Sonar transducer analysis and optimization using the finite element method," Ph.D. Thesis, printed in University of Birmingham, Chapter 7, 1991.
7. L. G. Copley, "Fundamental results concerning integral representations in acoustic radiation," *J. Acoust. Soc. Am.* **44**, 28-32, 1968.
8. E. Skudrzyk, "The foundation of acoustics," (Springer-Verlag, New York, 1971), 408-409, Equation (76), 1971.
9. D. T. I. Francis, "A boundary element method for the analysis of the acoustic field in three dimensional fluid-structure interaction problems," *Proc. Inst. of Acoust.*, **12**, Part 4, 76-84, 1990.
10. H. A. Schenck, "Improved integral formulation for acoustic radiation problems," *J. Acoust. Soc. Am.* **44**, 41-58, 1968.
11. A. J. Burton and G. F. Miller, "The application of integral integration methods to the numerical solutions of some exterior boundary problems," *Proc. R. Soc. London*, Ser. A 323, 201-210, 1971.
12. R. F. Kleinman and G. F. Roach, "Boundary integral equations for the three dimensional helmholtz equation," SIAM Rev., **16**, 214-236, 1974.
13. D. T. I. Francis, "A gradient formulation of the Helmholtz integral equation for acoustic radiation and scattering," *J. Acoust. Soc. Am.* **93** (4) Part 1, 1700-1709, 1993.
14. ALGOR, http://www.algor.com , ALGOR Inc.
15. S. S., Jarng. "Comparison of piezoelectric flextentional sonar transducer simulations between a coupled FE-BEM and ATILA code," *J. of Korean Ins. of Maritime Info. & Comm.*, **3** (3), 559-567, 1999.

[Profile]

• Soon-Suck Jarng

1984. 2: Hanyang Uni. (S. Korea), Dept. of Electronics (B.Eng.)
1985. 9: Hull Uni. (U.K.), Dept. of Electronics (M. Eng.)
1988. 9: Birmingham Uni. (U.K.), Dept. of Physiology (M.Sc.)
1991. 12: Birmingham Uni. (U.K.), Dept. of Electronic Electrical Eng. (Ph.D.)
1992. 3~Present: Chosun Uni. (S. Korea), Dept. of Information Control & Instrumentation

※ Main Research: Cochlear Bio-mechanics, Underwater/Underground Acoustics, Piezoelectric Sensor Device, Finite Element Method (FEM), Boundary Element Method (BEM)

• Je-Hyung Lee

1997. 2: Chosun Uni. (S. Korea), Dept. of Information Control & Instrumentation (B.Eng.)1999.9: Chosun Uni. (S. Korea), Dept. of Information Control & Instrumentation (M.Eng.)
1999.9~Present: Chosun Uni. (S. Korea), Dept. of Information Control & Instrumentation (Ph.D Student)